

Specific heat jump at the superconducting transition temperature in $\text{Ba}(\text{Fe}_{1-x}\text{Co}_x)_2\text{As}_2$ and $\text{Ba}(\text{Fe}_{1-x}\text{Ni}_x)_2\text{As}_2$ single crystals

Sergey L. Bud'ko, Ni Ni, and Paul C. Canfield

*Ames Laboratory US DOE and Department of Physics and Astronomy,
Iowa State University, Ames, IA 50011, USA*

(Dated: February 12, 2022)

Abstract

We present detailed heat capacity measurements for $\text{Ba}(\text{Fe}_{1-x}\text{Co}_x)_2\text{As}_2$ and $\text{Ba}(\text{Fe}_{1-x}\text{Ni}_x)_2\text{As}_2$ single crystals in the vicinity of the superconducting transitions. The specific heat jump at the superconducting transition temperature (T_c), $\Delta C_p/T_c$, changes by a factor ~ 10 across these series. The $\Delta C_p/T_c$ vs. T_c data of this work (together with the literature data for $\text{Ba}(\text{Fe}_{0.939}\text{Co}_{0.061})_2\text{As}_2$, $(\text{Ba}_{0.55}\text{K}_{0.45})\text{Fe}_2\text{As}_2$, and $(\text{Ba}_{0.6}\text{K}_{0.4})\text{Fe}_2\text{As}_2$) scale well to a single log-log plot over two orders of magnitude in $\Delta C_p/T_c$ and over about an order of magnitude in T_c , giving $\Delta C_p/T_c \propto T_c^2$.

PACS numbers: 74.25.Bt, 74.62.Dh, 74.70.Dd

The discovery of superconductivity in F-doped LaFeAsO^1 and K-doped $\text{BaFe}_2\text{As}_2^2$ compounds resulted in a large number of experimental and theoretical studies of the materials containing Fe-As layers as a structural unit. The understanding that transition metal (TM) substitution for Fe in the $(\text{AE})\text{Fe}_2\text{As}_2$ series ($\text{AE} = \text{Ba}, \text{Sr}, \text{Ca}$) could be used to both stabilize superconductivity^{3,4,5} and simplify growth while improving homogeneity, makes the $(\text{AE})(\text{Fe}_{1-x}\text{TM}_x)_2\text{As}_2$ series (and in particular $\text{Ba}(\text{Fe}_{1-x}\text{TM}_x)_2\text{As}_2^{3,6,7,8,9,10}$) a model system for studies of physical properties of Fe-As based materials.

Despite the large experimental and theoretical effort to understand the nature of superconductivity in Fe-As based materials, there are still a number of open issues that have not been well resolved. From the experimental point of view, for number of properties, either the spread in the data is large, or systematic sets of data are absent. Temperature-dependent specific heat measured through the superconducting transition is one such property, even though it is considered to reflect of the superconductivity mechanism. Apart from the functional dependence of the specific heat ($C_p(T)$) below the superconducting transition temperature (T_c), the study of which often has complications caused by the need of careful subtraction of the normal state contributions, the size of jump in C_p at the superconducting transition is known to depend on the details of the superconducting state^{11,12,13,14}, as judged and modeled by its deviation from the isotropic, weak coupling, BCS value of $\Delta C_p/\gamma T_c = 1.43$ (γ being the normal state electronic specific heat).

The $\text{Ba}(\text{Fe}_{1-x}\text{Co}_x)_2\text{As}_2$ and $\text{Ba}(\text{Fe}_{1-x}\text{Ni}_x)_2\text{As}_2$ families of materials share very similar and complex $x - T$ phase diagrams^{7,8,10}: initially on Co(Ni) -doping the critical temperature of the structural/antiferromagnetic transition decreases, with a separation in critical temperatures between these two transitions,^{15,16} then, above some critical concentration, superconductivity is observed, apparently in the orthorhombic/antiferromagnetic phase. At higher Co(Ni) concentrations the structural/magnetic transitions are fully suppressed, whereas superconductivity appears to persist in the tetragonal phase up to $x \sim 0.14$ for $\text{TM} = \text{Co}$ and $x \sim 0.08$ for $\text{TM} = \text{Ni}$. In this work we study the evolution of the specific heat jump at T_c with $\text{TM} = \text{Co}$ and Ni doping, for different concentration of TM . We examine the whole superconducting dome (both in orthorhombic/antiferromagnetic and tetragonal low temperature phases of the $x - T$ diagram) to gain insight into the details of the superconducting state in these materials.

Single crystals of $\text{Ba}(\text{Fe}_{1-x}\text{Co}_x)_2\text{As}_2$ and $\text{Ba}(\text{Fe}_{1-x}\text{Ni}_x)_2\text{As}_2$ were grown out of self flux using conventional high-temperature solution growth techniques.¹⁷ Detailed description of the crystal growth procedure for this series can be found elsewhere.^{7,10} The samples are plate-like with the plates being perpendicular to the crystallographic c -axis. The heat capacity data on the samples were measured using a hybrid adiabatic relaxation technique of the heat capacity option in a Quantum Design, PPMS instrument. Part of the $C_p(T)$ data for $\text{Ba}(\text{Fe}_{1-x}\text{Co}_x)_2\text{As}_2$ were presented, but not analyzed in detail, in Ref. 7.

It has to be noted, that both the superconducting transition temperatures and the upper critical fields in these materials are rather high⁷, thus making a reliable estimate of the normal state electronic specific heat, γ , difficult, especially bearing in mind that for approximately half of the samples in this study superconductivity coexists with an antiferromagnetic long range order. For this reason we are limited to the experimental determination of $\Delta C_p/T_c$, rather than the more traditional quantity $\Delta C_p/\gamma T_c$. Due to finite widths of the superconducting transitions, $\Delta C_p/T_c$ and T_c values were determined from plots of C_p/T vs. T using an "isoentropic" construction (Fig. 1(b), inset). So defined values of T_c may be slightly smaller than those reported for the samples from the same batches in Refs. [7,10] in which different criterion was used.

Temperature dependent heat capacity data for $\text{Ba}(\text{Fe}_{1-x}\text{Co}_x)_2\text{As}_2$ and $\text{Ba}(\text{Fe}_{1-x}\text{Ni}_x)_2\text{As}_2$, plotted as C_p/T vs. T^2 are shown in Figs. 1(a),(b). The jumps associated with the superconducting transitions are seen for all concentrations presented. Fig. 1(c) presents all of the $C_p(T)$ data together showing that the spread of the data above the superconducting transitions is small, within 5-6%, consistent with simple sample weighting errors. In addition, Fig. 1(c) shows that both Co and Ni, added in these small amounts, are small perturbations to the BaFe_2As_2 system and do not significantly change the background C_p .

The values of the specific heat jumps at superconducting transition in the form of $\Delta C_p/T_c$ are plotted as a function of TM = Co, Ni concentration in Fig. 2. The values of T_c as a function of x are displayed on the same plots as well. It is remarkable that (i) $\Delta C_p/T_c$ values change by as much as a factor of ~ 10 for the samples within the series; (ii) the shapes of the C_p/T_c vs. x curves for both series appear to be related to the shapes of the respective T_c vs. x superconducting domes.

These data can be plotted as $\Delta C_p/T_c$ vs. T_c (Fig. 3). It is curious, that all the data (both

for "underdoped" and "overdoped" parts of the superconducting dome) collapse rather well onto a single curve. A data point⁸ from another group's work on $\text{Ba}(\text{Fe}_{0.939}\text{Co}_{0.061})_2\text{As}_2$ is consistent with our data, moreover, our previous result¹⁸ on $\text{Ba}_{0.55}\text{K}_{0.45}\text{Fe}_2\text{As}_2$ as well as the very large C_p jump at superconducting transition reported for $\text{Ba}_{0.6}\text{K}_{0.4}\text{Fe}_2\text{As}_2$ [19,20] follow the same trend (Fig. 3). All the data in this figure can be fitted by a straight line with a slope $n \approx 2$.

There are several possible ways to address such a remarkable behavior.

Inhomogeneities: it has been known that in a few cases (e.g. K-doping in BaFe_2As_2 samples^{18,21} the resulting samples had a distribution of dopant concentration, resulting in a broadening of the phase transitions. It appears to be less the case for TM doping: the wavelength dispersive x-ray spectroscopy does not show unambiguous, beyond the instrument error bars, distribution of TM dopant^{7,10,22}, for the more studied $\text{Ba}(\text{Fe}_{1-x}\text{Co}_x)_2\text{As}_2$ series, the low field susceptibility does not show variation in either transition width or magnetic flux expulsion,⁷ Meissner screening is homogeneous,²³, structural and antiferromagnetic transitions for the intermediate concentrations are reasonably sharp^{7,15,24}, and, for the phase diagrams and several other properties, results from the different groups appear to be very close.^{7,8} This being said, in an oversimplified model, inhomogeneities can be modeled by a uniform distribution of superconducting transition temperatures within some temperature range. For an aggressive, $\pm 10\%$ of T_c spread, the width of the distribution (using $x = 0.074$ Co data as a starting point), the apparent $\Delta C_p/T_c$ jump will be approximately factor of 3 (but not ~ 10) smaller than the initial one, thus suggesting that inhomogeneity is not the sole reason for the observed behavior. In addition, the fact that the data in Fig. 3 are linear, with a slope $n \approx 2$, over two orders of magnitude in $\Delta C_p/T_c$ and over about an order of magnitude in T_c on a log-log plot argues against an artifact caused by an uncontrolled spread in composition and may imply some more profound physical mechanism.

Significant change of the density of states within small, $\sim 10\%$ range TM = Co, Ni doping, with $\gamma(x)$ or $DOS(x)$ having dome-like shape centered at x values corresponding to the observed maximum in T_c : in this case $\Delta C_p/\gamma T_c$ could be close to constant or change insignificantly, whereas strongly x -dependent $\Delta C_p/T_c$ will be observed. Although, as mentioned above, reliable experimental data on normal state electronic specific heat as a function of x are not available, band structure calculations on pure BaFe_2As_2 ^{25,26,27} do not suggest such

a significant and *non-monotonic* change of the density of states for small TM = Co, Ni concentrations (a sharp local maximum in γ would be required at optimal doping).

More physical reasons to observe significant change (decrease in comparison with isotropic, weak coupling, BCS case) in the heat capacity jump at T_c could be associated with the effect of paramagnetic impurities,¹² multi-band superconductivity,^{13,14} and/or effects of a normal state pseudogap.²⁸ Although each of these possibilities is plausible and exciting, it seems hard to construct a simple picture that will accommodate the observed dome-like, almost symmetric, $\Delta C_p/T_c$ vs. x behavior within a single one of this models (unless a more complex case, in which left and right, "underdoped" and "overdoped", parts of the $\Delta C_p/T_c$ vs. x dome, are explained separately by different mechanism, is considered).

To summarize, approximate scaling of $\Delta C_p/T_c$ with T_c was observed for $\text{Ba}(\text{Fe}_{1-x}\text{Co}_x)_2\text{As}_2$ and $\text{Ba}(\text{Fe}_{1-x}\text{Ni}_x)_2\text{As}_2$ single crystals. The reason for such scaling is not clear in this moment: if extrinsic (chemical inhomogeneities) it cannot be ignored in interpretation of other, detailed, experiments on these materials, if intrinsic, more work is required to elucidate the reason for this apparent scaling.

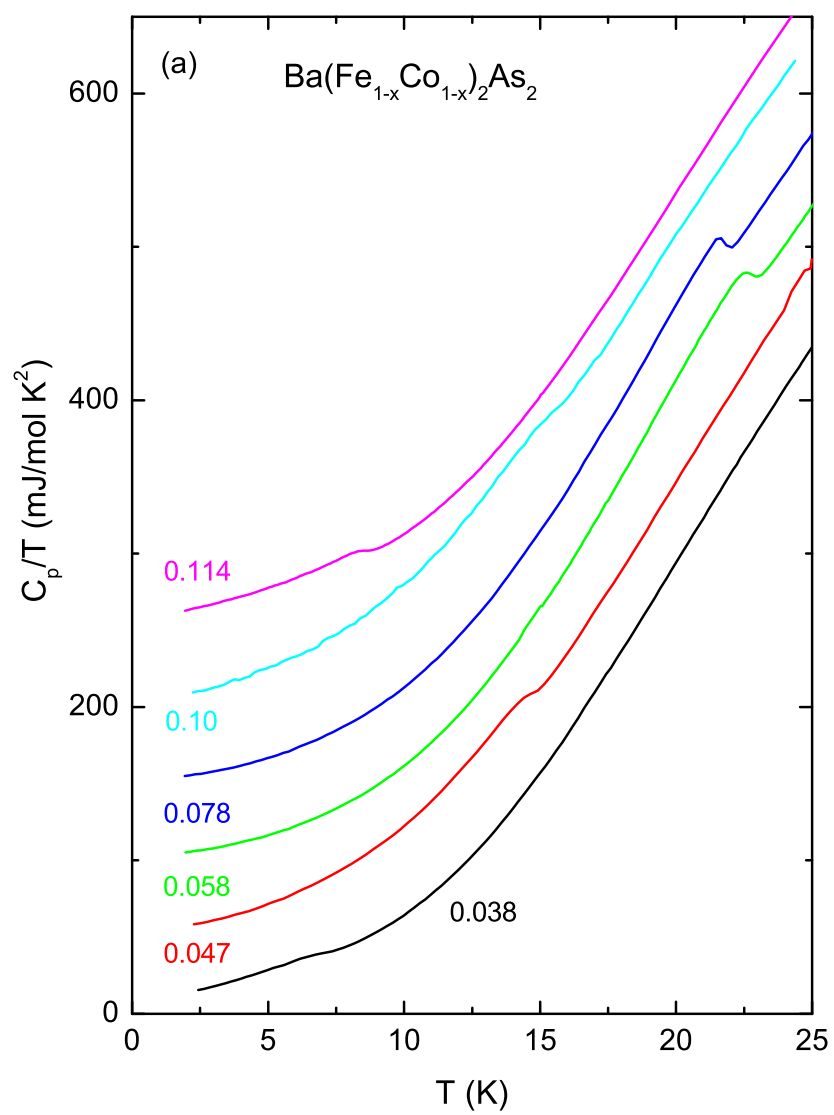
Acknowledgments

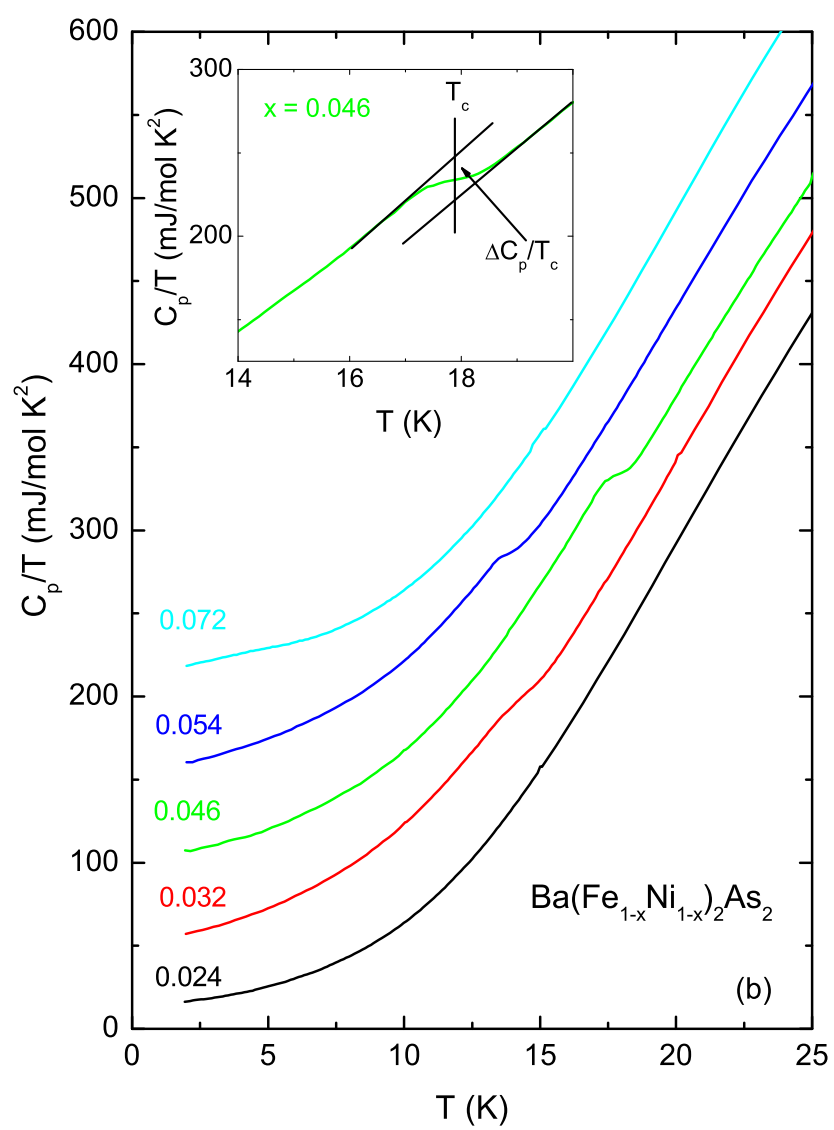
Work at the Ames Laboratory was supported by the US Department of Energy - Basic Energy Sciences under Contract No. DE-AC02-07CH11358. We thank Vladimir Kogan and Jörg Schmalian for useful discussions and Jiaqiang Yan for help in synthesis.

-
- ¹ Y. Kamihara, T. Watanabe, M. Hirano, H. Hosono, Journal of the American Chemical Society **130**, 3296 (2008).
 - ² Marianne Rotter, Marcus Tegel, and Dirk Johrendt, Phys. Rev. Lett. **101**, 107006 (2008).
 - ³ Athena S. Sefat, Rongying Jin, Michael A. McGuire, Brian C. Sales, David J. Singh, and David Mandrus, Phys. Rev. Lett., **101**, 117004 (2008).
 - ⁴ A. Leithe-Jasper, W. Schnelle, C. Geibel, and H. Rosner, Phys. Rev. Lett. **101**, 207004 (2008).
 - ⁵ Neeraj Kumar, R. Nagalakshmi, R. Kulkarni, P. L. Paulose, A. K. Nigam, S. K. Dhar, and A. Thamizhavel, Phys. Rev. B **79**, 012504 (2009).

- ⁶ K. Ahilan, J. Balasubramaniam, F. L. Ning, T. Imai, A. S. Sefat, R. Jin, M. A. McGuire, B. C. Sales, and D. Mandrus, *J. Phys.: Condens. Matter* **20**, 472201 (2008).
- ⁷ N. Ni, M. E. Tillman, J.-Q. Yan, A. Kracher, S. T. Hannahs, S. L. Bud'ko, and P. C. Canfield, *Phys. Rev. B* **78**, 214515 (2008).
- ⁸ Jiun-Haw Chu, James G. Analytis, Chris Kucharczyk, and Ian R. Fisher, *Phys. Rev. B* **79**, 014506 (2009).
- ⁹ L. J. Li, Y. K. Luo, Q. B. Wang, H. Chen, Z. Ren, Q. Tao, Y. K. Li, X. Lin, M. He, Z. W. Zhu, G. H. Cao, and Z. A. Xu, *New J. Phys.* **11**, 025008 (2009).
- ¹⁰ P. C. Canfield, S. L. Bud'ko, Ni Ni, J. Q. Yan, and A. Kracher, arXiv:0904.3134v1, unpublished.
- ¹¹ J. P. Carbotte, *Rev. Mod. Phys.* **62**, 1027 (1990).
- ¹² S. Skalski, O. Betbeder-Matibet, and P. R. Weiss, *Phys. Rev.* **136**, A1500 (1964).
- ¹³ Todor M. Mishonov, Evgeni S. Penev, Joseph O. Indekeu, and Valery L. Pokrovsky, *Phys. Rev. B* **68**, 104517 (2003).
- ¹⁴ V. G. Kogan, C. Martin, and R. Prozorov, arXiv:0905.0029v1, unpublished.
- ¹⁵ D. K. Pratt, W. Tian, A. Kreyssig, J. L. Zarestky, S. Nandi, N. Ni, S. L. Budko, P. C. Canfield, A. I. Goldman, and R. J. McQueeney, arXiv:0903.2833v1, unpublished.
- ¹⁶ C. Lester, Jiun-Haw Chu, J. G. Analytis, S. C. Capelli, A. S. Erickson, C. L. Condon, M. F. Toney, I. R. Fisher, and S. M. Hayden, *Phys. Rev. B* **79**, 144523 (2009).
- ¹⁷ P. C. Canfield, Z. Fisk, *Phil. Mag. B* **65**, 1117 (1992).
- ¹⁸ N. Ni, S. L. Bud'ko, A. Kreyssig, S. Nandi, G. E. Rustan, A. I. Goldman, S. Gupta, J. D. Corbett, A. Kracher, and P. C. Canfield, *Phys. Rev. B* **78**, 014507 (2008).
- ¹⁹ U. Welp, R. Xie, A. E. Koshelev, W. K. Kwok, H. Q. Luo, Z. S. Wang, G. Mu, and H. H. Wen, *Phys. Rev. B* **79**, 094505 (2009).
- ²⁰ Gang Mu, Huiqian Luo, Zhaosheng Wang, Lei Shan, Cong Ren, and Hai-Hu Wen, *Phys. Rev. B* **79**, 174501 (2009).
- ²¹ A. A. Aczel, E. Baggio-Saitovitch, S. L. Bud'ko, P. C. Canfield, J. P. Carlo, G. F. Chen, Pengcheng Dai, T. Goko, W. Z. Hu, G. M. Luke, J. L. Luo, N. Ni, D. R. Sanchez-Candela, F. F. Tafti, N. L. Wang, T. J. Williams, W. Yu, and Y. J. Uemura, *Phys. Rev. B* **78**, 214503 (2008).
- ²² N. Ni, et al., in preparation.
- ²³ R. T. Gordon, C. Martin, H. Kim, N. Ni, M. A. Tanatar, J. Schmalian, I. I. Mazin, S. L. Bud'ko, P. C. Canfield, and R. Prozorov, *Phys. Rev. B* **79**, 100506 (2009).

- ²⁴ S. L. Bud'ko, N. Ni, S. Nandi, G. M. Schmiedeshoff, and P. C. Canfield, Phys. Rev. B **79**, 054525 (2009).
- ²⁵ I.R. Shein, A.L. Ivanovskii, Pis'ma v ZhETF **88**, 115 (2008).
- ²⁶ C. Krellner, N. Caroca-Canales, A. Jesche, H. Rosner, A. Ormeci, and C. Geibel, Phys. Rev. B **78**, 100504 (2008).
- ²⁷ C. Liu, G. D. Samolyuk, Y. Lee, N. Ni, T. Kondo, A. F. Santander-Syro, S. L. Bud'ko, J. L. McChesney, E. Rotenberg, T. Valla, A. V. Fedorov, P. C. Canfield, B. N. Harmon, and A. Kaminski, Phys. Rev. Lett. **101**, 177005 (2008)
- ²⁸ J. W. Loram, J. Luo, J. R. Cooper, W. Y. Liang, and J. L. Tallon, J. Phys. Chem. Solids **62**, 59 (2001).





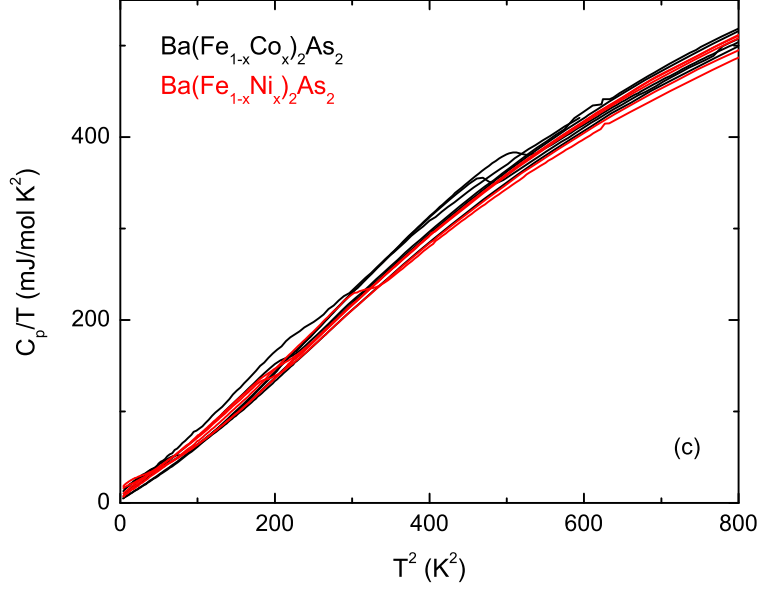


FIG. 1: (Color online) Temperature-dependent specific heat of (a) $\text{Ba}(\text{Fe}_{1-x}\text{Co}_x)_2\text{As}_2$, (b) $\text{Ba}(\text{Fe}_{1-x}\text{Ni}_x)_2\text{As}_2$ single crystals plotted as C_p/T vs. T . Inset to panel (b): enlarged C_p/T vs. T plot near the superconducting transition for $\text{Ba}(\text{Fe}_{0.954}\text{Ni}_{0.046})_2\text{As}_2$, lines show how T_c and $\Delta C_p/T_c$ are estimated. Data in panels (a) and (b) are shifted by a multiple of 50 mJ/mol K² along the y - axis for clarity. Panel (c): data for both series plotted as C_p/T vs. T^2 without shifts.

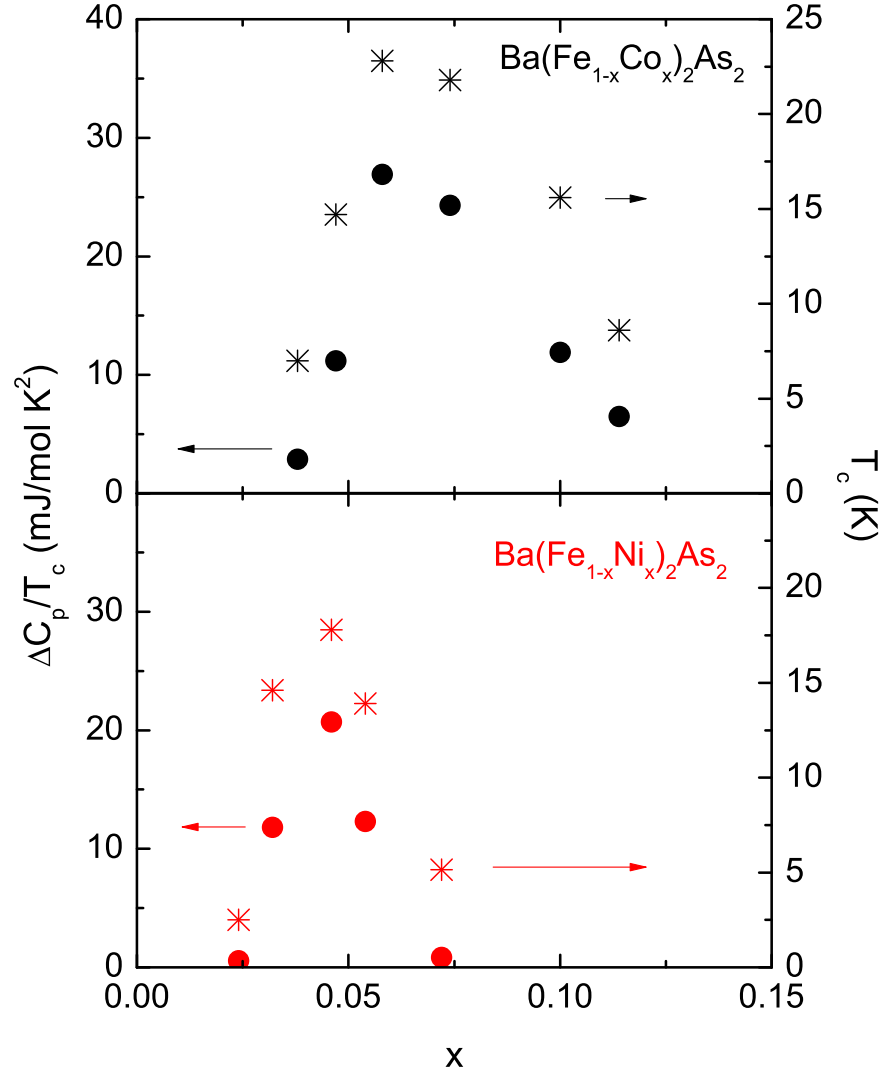


FIG. 2: (Color online) $\Delta C_p / T_c$ (circles, left axis) and T_c (asterisks, right axis) as a function of concentration, x , $\text{Ba}(\text{Fe}_{1-x}\text{Co}_x)_2\text{As}_2$ (upper panel) and $\text{Ba}(\text{Fe}_{1-x}\text{Ni}_x)_2\text{As}_2$ (lower panel).

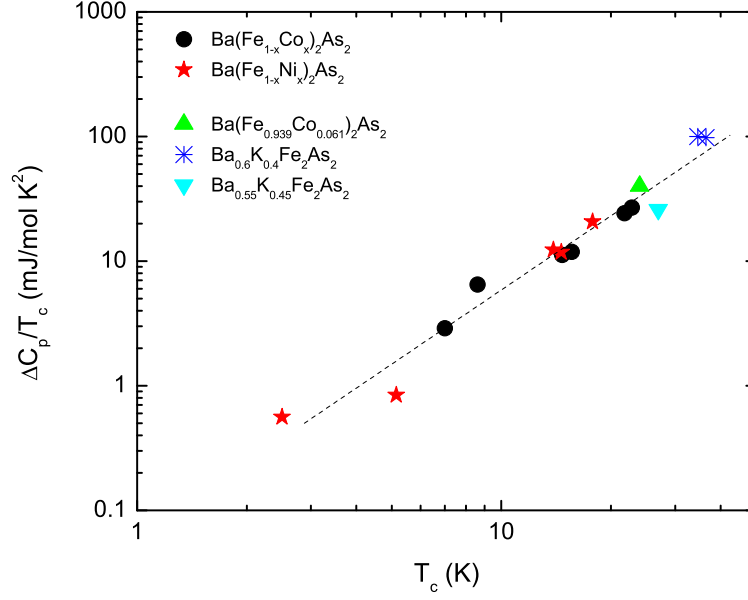


FIG. 3: (Color online) $\Delta C_p/T_c$ vs. T_c for $\text{Ba(Fe}_{1-x}\text{Co}_x)_2\text{As}_2$ (circles) and $\text{Ba(Fe}_{1-x}\text{Ni}_x)_2\text{As}_2$ (stars) plotted together with literature data for $\text{Ba(Fe}_{0.939}\text{Co}_{0.061})_2\text{As}_2$ [8], $\text{Ba}_{0.55}\text{K}_{0.45}\text{Fe}_2\text{As}_2$ [18], and $\text{Ba}_{0.6}\text{K}_{0.4}\text{Fe}_2\text{As}_2$ [19,20]. Dashed line has a slope $n = 2$ and is a guide for the eye.